JACS
JOURNAL OF THE AMERICAN CHEMICAL SOCIETY
COMMUNICATION
pubs.acs.org/JACS

Electronically Regulated Thermally and Light-Gated Electron Transfer from Anions to Naphthalenediimides

Samit Guha, Flynt S. Goodson, Sovan Roy, Lucas J. Corson, Curtis A. Gravenmier, and Sourav Saha*

Department of Chemistry and Biochemistry and Integrative NanoScience Institute, Florida State University,
95 Chieftan Way, Tallahassee, Florida 32306-4390, United States

S *Supporting Information*

ABSTRACT: Anion-induced electron transfer (ET) to π-electron-deficient naphthalenediimides (NDIs) can be channeled through two distinct pathways by adjusting the Lewis basicity of the anion and the π-acidity of the NDI: (1) When the anion and NDI are a strong electron donor and acceptor, respectively, positioning the HOMO of the anion above the LUMO of the NDI, a thermal anion → NDI ET pathway is turned ON. (2) When the HOMO of a weakly Lewis basic anion falls below the LUMO of an NDI but still lies above its HOMO, the thermal ET is turned OFF, but light can activate an unprecedented anion → ^{1}*NDI photoinduced ET pathway from the anion's HOMO to the photogenerated ^{1}*NDI's SOMO−1. Both pathways generate NDI$^{•-}$ radical anions.

Although anion-induced electron transfer (ET) is found in nature (e.g., ascorbate reduces cytochromes *b* and *c*),[1] anion-mediated charge transfer (CT)[2] and, especially, formal ET[3] to neutral π-acceptors analogous to π-donor/acceptor interactions[4] are extremely rare. To display anion/π-acceptor[5] and anion-induced CT[2] and ET[3] interactions, the π-acceptors must possess strong electron-accepting abilities, low LUMO (π*) levels, and large positive quadrupole moments.

1,4,5,8-Naphthalenediimides (NDIs) are π-electron-deficient colorless compounds (Scheme 1a) with easily tunable electronic properties.[6] Although π-donor/acceptor CT interactions of NDIs are well-known,[4] anion → NDI CT and ET interactions have remained unexplored until recently. In 2010, Matile and co-workers[2b] reported extremely weak CT interactions between polarizable anions (Br^- and I^-) and π-acidic NDIs, while we[3] discovered a unique formal ET from strongly Lewis basic F^- to an NDI that generated an NDI$^{•-}$ radical anion. Herein we demonstrate for the first time that by adjustment of the π-acidity (LUMO levels) of NDIs with respect to the Lewis basicity (HOMO levels) of anions, anion → NDI ET processes can be channeled through two distinct pathways (Scheme 1), both of which generate NDI$^{•-}$ radical anions: (1) When the HOMO of an anion is located above the LUMO of an NDI, a thermal anion → NDI ET takes place from the anion's HOMO to the NDI's LUMO (Scheme 1c). (2) When the HOMO of an anion lies below the LUMO of an NDI receptor but above its HOMO, the thermal anion → NDI ET is turned OFF, but light can activate an unprecedented anion → ^{1}*NDI photoinduced ET (PET) pathway from the anion's HOMO to the photogenerated ^{1}*NDI's SOMO−1 (Scheme 1d). Weak CT interactions take place between strongly π-acidic NDIs and weakly Lewis basic but highly polarizable anions. We also put forth two other possible mechanisms for chromogenic anion/NDI interactions—nucleophilic attack of the anion on the NDI to form covalent intermediates[5d,7] and CH···anion interactions[8] with the NDI's core protons—and demonstrate how the experimental results not only rule out these scenarios but also confirm the ET and PET phenomena.

Scheme 1. (a, b) Illustrations of (a) Thermal Anion → NDI ET Interactions from Strongly Lewis Basic Anions to Strongly π-Acidic NDIs and (b) Anion → ^{1}*NDI PET from Less Basic Anions to NDIs That Show Weak or No Thermal ET; (c, d) Energy Level Diagrams of (c) Thermal ET and (d) PET Events

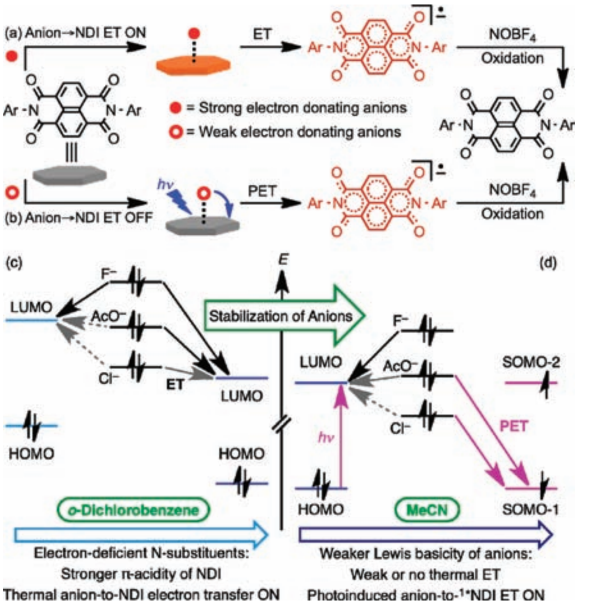

While π-acidification of NDIs using electron-withdrawing core substituents has been achieved,[6b] little is known about the effects of imide N-substituents on the electronic and anion-recognition properties. Herein we show how electron-rich and -deficient N-substituents impact the π-acidity of NDIs and regulate their anion-recognition properties with remarkable precision. To study the relationships between the π-acidity of NDIs and the anion/NDI interactions, we installed electron-deficient (in **1**−**4**) or electron-rich (in **6** and **7**) groups on the imide N-centers and compared the resulting NDIs with reference NDI **5** (Chart 1). These NDIs were prepared by bisimidization of

Received: June 16, 2011
Published: August 30, 2011

dx.doi.org/10.1021/ja2055726 | *J. Am. Chem. Soc.* 2011, 133, 15256–15259

Table 1. NDI Redox Potentials (vs Ag/AgCl in MeCN), HOMO and LUMO Energies, and Thermal and Photoinduced Anion → NDI ET in ODCB and MeCN

Symmetric NDI receptors with electron-deficient and -rich *N,N'*-diaryl substituents	E^1_{Red} / E^2_{Red} (mV)	LUMO/ HOMO (eV)	ODCB				MeCN			
			F^-	AcO^-	$H_2PO_4^-$	Cl^-	F^-	AcO^-	$H_2PO_4^-$	Cl^-
1. *N,N'*-Bis(2,6-diiodo-4-nitrophenyl) NDI	−310/−790	−4.07/−7.17	✅	✅	☑ $h\nu$↑	☑ $h\nu$↑	✅	☑ $h\nu$↑	☑ $h\nu$↑	☒ $h\nu$↑
2. *N,N'*-Bis(2,6-difluorophenyl) NDI	−380/−830	−4.00/−7.10	✅	✅	☑ $h\nu$↑	☒	✅	☑ $h\nu$↑	☑ $h\nu$↑	☒
3. *N,N'*-Bis(2,6-diiodo-4-methylphenyl) NDI	−395/−885	−3.98/−7.08	✅	✅	☑ $h\nu$↑	☒	✅	☒ $h\nu$↑	☒ $h\nu$↑	☒
4. *N,N'*-Di(4-nitrophenyl) NDI	−510/−900	−3.87/−6.97	✅	✅	☑ $h\nu$↑	☒	✅	☒ $h\nu$↑	☒ $h\nu$↑	☒
5. *N,N'*-Diphenyl NDI	−535/−965	−3.85/−6.95	✅	✅	☒ $h\nu$↑	☒	✅	☒	☒	☒
6. *N,N'*-Di(4-anisyl) NDI	−550/−975	−3.83/−6.93	✅	☑ $h\nu$↑	☒	☒	✅	☒	☒	☒
7. *N,N'*-Di(4-tolyl) NDI	−560/−980	−3.82/−6.92	✅	☑ $h\nu$↑	☒	☒	✅	☒	☒	☒

[a] Legend: ✅: strong thermal anion→NDI ET interactions; ☑: weak thermal anion→NDI ET interactions; ☒: thermal anion→NDI ET OFF; $h\nu$↑: anion → ^{1*}NDI PET ON. Calculations of HOMO and LUMO energies: $\Delta E_{HOMO/LUMO} = [1240/(\lambda_{max(onset)}\text{ in nm})]$ eV; $E_{LUMO} = [-4.8 - E^1_{Red} - 0.42)]$ eV for E^1_{Red} in V vs Ag/AgCl; $E_{HOMO} = E_{LUMO} - \Delta E_{HOMO/LUMO}$ eV.[6b]

Chart 1. Molecular Structures of NDIs 1−7

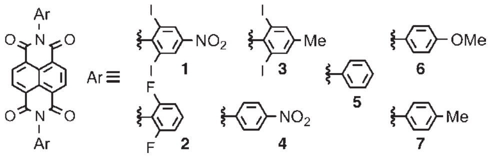

naphthalene-1,4,5,8-tetracarboxydianhydride with the appropriate amines (Scheme S1 in the Supporting Information).[6]

NDIs **1**−**7** display nearly identical UV absorption spectra (λ = 340−390 nm) (Figures S1 and S2), indicating that the N-substituents do not affect the HOMO−LUMO energy gaps. These NDIs undergo two reversible one-electron reductions (Figure S3), forming $NDI^{\bullet-}$ and NDI^{2-} species.[3,6,9] The electron-deficient *N*-aryl substituents enhance the π-acidity of NDIs **1**−**4**, as evidenced by their smaller reduction potentials and lower LUMO levels relative to NDI **5**. The electron-rich N-substituents suppress the π-acidity of NDIs **6** and **7**, as they possess more negative reduction potentials and higher LUMO levels. Electrochemical reduction of NDIs to $NDI^{\bullet-}$ radical anions produces highly featured absorption spectra with prominent peaks at ca. 475 (λ_{max}), 605, 700, and 800 nm and establishes a clear isosbestic point at ca. 390 nm (Figure 1a and Figure S4).[3,9] The HOMO and LUMO energies of NDIs **1**−**7** and their anion-recognition phenomena through thermal and photoinduced ET pathways are summarized in Table 1.

To understand the effects of the NDI's π-acidity and the anion's electron-donating ability (as reflected by the anion's Lewis basicity and oxidation potential[10]) on the anion → NDI ET phenomena, we surveyed the interactions between NDIs **1**−**7** and tetra-*n*-butylammonium (TBA^+) salts of F^-, AcO^-, $H_2PO_4^-$, Cl^-, Br^-, I^-, and PF_6^-. To prevent the solvent from acting as an electron donor and to determine the effect of the solvent on the anion/NDI interactions, we conducted our studies in *o*-dichlorobenzene (ODCB) and MeCN. The π-acidity of NDIs **1**−**7** follows the same trend in these two solvents, but most NDIs have slightly stronger π-acidity in MeCN, as shown by cyclic voltammetry (Figure S3). While the absorption features of electrochemically generated $NDI^{\bullet-}$ are essentially the same in the two solvents, the λ_{max} (ca. 475 nm) and isosbestic point (ca. 390 nm) appear at slightly shorter wavelengths (by ca. 8 nm) in MeCN than in ODCB (Figure S5).

UV/Vis titrations of NDIs **1**−**7** in ODCB with Lewis basic F^- display prominent $NDI^{\bullet-}$ spectra (Figure 1c and Figure S4). As the π-acidity of the NDI gradually diminishes in going from **1** to **7**, the extent of $NDI^{\bullet-}$ formation decreases (Figure 1c). This trend suggests that the thermal F^- → NDI ET diminishes as the energy gap between the anion's HOMO and the NDI's LUMO (ΔG°_{ET}) gradually decreases (Scheme 1c,d) with the fading π-acidity. On the other hand, as the Lewis basicity of the anions decreases ($F^- > AcO^- > H_2PO_4^- > Cl^-$),[10] their electron-donating abilities and HOMO levels diminish,[2c] weakening and eventually turning OFF the

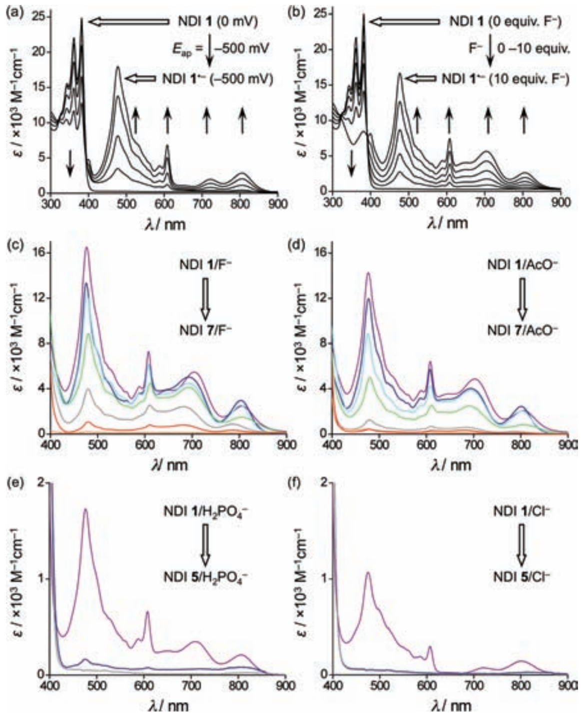

Figure 1. (a, b) UV/Vis spectroscopic changes of NDI **1** as a result of (a) electrochemical reduction (applied voltage E_{ap} = −500 mV vs Ag/AgCl, 0.1 M $TBAPF_6$/ODCB) and (b) titration with F^- (0−10 equiv), demonstrating the formation of $\mathbf{1}^{\bullet-}$ in both cases. (c−f) Anion-generated UV/Vis spectra of $NDI^{\bullet-}$ radical anions of NDIs **1** (violet), **2** (indigo), **3** (cyan), **4** (green), **5** (gray), **6** (orange), and **7** (red) (each 30 μM in ODCB) in the presence of (c) F^- (10 equiv), (d) AcO^- (50 equiv), (e) $H_2PO_4^-$ (50 equiv), and (f) Cl^- (100 equiv). The spectra show that while (c) F^- and (d) AcO^- generate the $NDI^{\bullet-}$ radical anions of **1**−**7**, (e) $H_2PO_4^-$ does so only for **1** and **2** and (f) Cl^- only for NDI **1**.

thermal ET (Scheme 1). As a result, in ODCB, less basic AcO^- generates weaker $NDI^{\bullet-}$ signals from NDIs **1**−**7** (Figure 1d) than those produced by F^-, while $H_2PO_4^-$ generates very weak $NDI^{\bullet-}$ signals only with NDIs **1**−**4** (Figure 1e) and Cl^- triggers extremely weak thermal ET only to NDI **1** (Figure 1f). The extent of $NDI^{\bullet-}$ formation via anion-induced thermal ET can be quantified by comparing the molar absorptivities (ε_{max} at ca. 475 nm) of the anion-generated and electrochemically generated $NDI^{\bullet-}$ (Figure 1 and Figure S4). Anion/NDI interactions between stronger electron donors and acceptors produce more $NDI^{\bullet-}$ radical anions and vice versa.

The anion-generated $NDI^{\bullet-}$ absorption spectra and isosbestic points are essentially identical to those of electrochemically generated $NDI^{\bullet-}$ radical anions in the absence of any electron-donating anions (Figure 1a,b and Figure S4). These similarities strongly suggest that anion → NDI ET events are indeed responsible for these spectroscopic changes and rule out the possibility of nucleophilic attack of anions on NDIs to form covalent intermediates,[5d,7] a scenario that would have produced UV/Vis spectra and isosbestic points different from those displayed by the electrochemically generated $NDI^{\bullet-}$ radical anions.

Treatment of the anion-induced absorption changes at 475 nm (λ_{max} of $NDI^{\bullet-}$) as a function of the NDI and anion concentrations using the Benesi−Hildebrand method[11] (Figure S6) shows a good agreement for 1:1 interactions between NDI **1** and F^-, AcO^-, and $H_2PO_4^-$ with gradually decreasing affinities (K_a = 1225, 70, and 40 M^{-1}, respectively, in ODCB at 298 K). Isothermal titration calorimetry (ITC) analyses (Figure S7) also show 1:1 interactions between F^- and NDIs **1**−**5** with gradually decreasing K_a values of 1230, 1080, 920, 710, and 530 M^{-1}, respectively (298 K, ODCB). Thus, K_a is greater for interactions between stronger Lewis basic anions and more π-acidic NDIs. Electrospray ionization mass spectrometry (ESI-MS) revealed several 1:1 NDI·anion complexes (see below).

In a more polar solvent, MeCN, strongly basic F^- generates $NDI^{\bullet-}$ absorption spectra of NDIs **1**−**7** via thermal ET (Figure S8), indicating that the HOMO of F^- is still located above the LUMOs of all these NDIs. However, less basic AcO^- and $H_2PO_4^-$ show significantly weaker ET interactions with only NDIs **1** and **2** (Figure 2a,b) that produce much less $NDI^{\bullet-}$ than in ODCB (Figure 1d,e). All Cl^- → NDI thermal ET processes are essentially turned OFF in MeCN, including that with the most π-acidic NDI, **1** (Figure 2c). The reducing abilities of less basic AcO^-, $H_2PO_4^-$, and Cl^- are further depleted through CH···anion interactions with MeCN,[8] which stabilize the HOMOs of these anions below the LUMOs of the weakly π-acidic NDIs, shutting down the thermal ET pathway (Scheme 1d).

We next explored whether a PET pathway[12] from the HOMO of an anion to the SOMO−1 of the ^{1*}NDI excited state (Scheme 1b, d) could turn ON the $NDI^{\bullet-}$ signal when the thermal anion → NDI ET process is turned OFF. To investigate this hypothesis, we used a W-lamp to irradiate NDI solutions containing anions that otherwise showed negligible or no thermal ET interactions in the dark and periodically recorded the UV/Vis spectra. Irradiation of a solution of **1** in MeCN in the presence of AcO^-, $H_2PO_4^-$, or Cl^-, which showed negligible or no thermal ET, immediately turned ON the anion → ^{1*}NDI PET, generating much stronger $NDI^{\bullet-}$ absorption spectra that reached saturation within 10 min of irradiation (Figure 2a−c). Similar PET phenomena were displayed by NDIs **2**−**4** with AcO^- and $H_2PO_4^-$ in MeCN (Figure S9).

Photoinduced enhancement of anion-mediated $NDI^{\bullet-}$ signals is also observed in ODCB when the thermal ET interactions are extremely weak or absent. For instance, AcO^- → ^{1*}NDI **6** (Figure 2d), $H_2PO_4^-$ → ^{1*}NDI **1**−**5**, and Cl^- → ^{1*}NDI **1** (Figure S10) PET signals are observed in ODCB. Interestingly, when a facile thermal anion → NDI ET process generates strong $NDI^{\bullet-}$ signals by directly populating the NDI's LUMO in the ground state (Scheme 1c,d), irradiation of these samples does not improve the $NDI^{\bullet-}$ signal intensity, indicating that the anion → ^{1*}NDI PET is turned OFF. On the other hand, when the thermal ET interactions are extremely weak or absent, the light-induced π → π* transition in the NDI opens the door for a more facile PET from the anion's HOMO to the ^{1*}NDI's SOMO−1 level (Scheme 1d). Less basic Br^-, I^-, and PF_6^- do not display any ET or PET to any of the NDIs in either solvent (Figure S11). However, a large excess of highly polarizable I^- produces a broad, weak CT band (λ_{CT} = 505 nm) with a concentrated solution (mM) of NDI **1** in ODCB but does not produce any $NDI^{\bullet-}$ (Figure S11a). Thus, by adjustment of the NDI's LUMO with respect to the anion's HOMO, the entire spectrum of ET, PET, and CT phenomena can be accessed. In control experiments, irradiation of these NDIs in the absence of anions did not produce any $NDI^{\bullet-}$ radical anion (Figures S1 and S2), ruling out the possibilities of intramolecular or solvent-mediated PET.

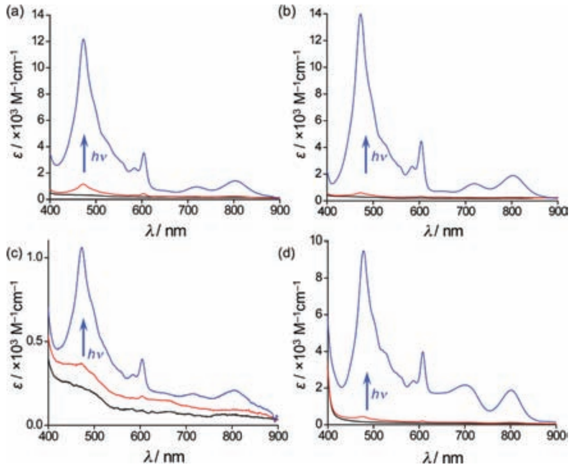

Figure 2. (a−c) UV/Vis spectra of NDI **1** (30 μM in MeCN, black traces) and of **1** with large excesses (≥50 equiv) of TBA^+ salts of (a) AcO^-, (b) $H_2PO_4^-$, and (c) Cl^- in the absence of light (red traces), showing extremely weak $NDI^{\bullet-}$ absorptions. (d) UV/Vis spectra of NDI **6** (30 μM in ODCB, black trace) and of **6** with excess AcO^- in the absence of light (red trace), showing negligible $NDI^{\bullet-}$ formation before irradiation. Irradiation of these solutions with a W-lamp (a−d) significantly enhanced the $NDI^{\bullet-}$ signals (blue traces), demonstrating the anion → ^{1*}NDI PET.

^1H NMR spectroscopy (CD_3CN) confirms that while F^-, AcO^-, and $H_2PO_4^-$ generate paramagnetic $\mathbf{1}^{\bullet-}$ through thermal ET, causing the NDI's core H_A signal to disappear (Figure 3a and Figure S12), Cl^- does not do so in the absence of light (Figure 3b). However, irradiation of the **1**/Cl^- sample quickly generates paramagnetic $\mathbf{1}^{\bullet-}$, as its H_A signal disappears. In contrast, less basic Br^- never produces any $NDI^{\bullet-}$ (Figure S12). The fact that the NDI's H_A signal does not split or shift from its original position before disappearing essentially rules out the formation of a nonsymmetric covalent NDI−anion intermediate via nucleophilic attack by anions[5d,7] or a CH··· anion interaction with the H_A protons.[8] The anion-generated $NDI^{\bullet-}$ radical anions are stable under dark, inert conditions. Oxidation of anion-generated $NDI^{\bullet-}$ with $NOBF_4$ regenerates the neutral NDIs, as the characteristic NMR signals return to their full glory (Figure 3a,b and Figure S12). The oxidative

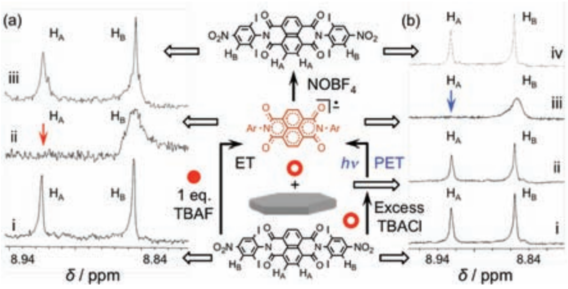

Figure 3. ^1H NMR spectra (CD_3CN, 298 K) of NDI **1** [trace i in (a) and (b)]; (a) **1** with 1 equiv of TBAF (trace ii) showing $\mathbf{1}^{\bullet-}$ formation via thermal ET, as indicated by the disappearance of the NDI's core H_A signal; and (b) **1** with excess TBACl before (trace ii) and after (trace iii) W-lamp irradiation, showing no $\mathbf{1}^{\bullet-}$ formation through thermal ET but $\mathbf{1}^{\bullet-}$ formation through PET, respectively. In both cases, $NOBF_4$ oxidation of $\mathbf{1}^{\bullet-}$ regenerated neutral NDI **1** [trace iii in (a) and trace iv in (b)].

regeneration of the NDI further indicates formation of the $NDI^{\bullet-}$ in the first place and provides additional evidence against NDI−anion covalent bond formation.

^{19}F NMR titration of NDI **2** with TBAF (Figure S13) shows a broadening and gradual disappearance of the NDI's F signals (−118.80 and −118.96 ppm), indicating the formation of paramagnetic $\mathbf{2}^{\bullet-}$. Conversely, titration of TBAF with NDI **2** shows a broadening and gradual upfield shift of the F^- signal (−117.2 ppm), indicating possible shielding of F^- by NDI **2** as a result of anion/NDI complex formation. The TBAF signal disappears completely with 1 equiv of NDI, indicating $F^\bullet$ formation via the thermal $F^- \rightarrow$ NDI ET process. EPR spectroscopy confirmed the formation of paramagnetic $NDI^{\bullet-}$ using F^- by displaying excellent agreement between the F^--generated and simulated $NDI^{\bullet-}$ spectra (Figure S14).[3]

ESI-MS (Figure S15) reveals the complexes $\mathbf{1}\cdot F^-$ (m/z 1030.9), $\mathbf{1}\cdot AcO^-$ (1070.7), $\mathbf{1}\cdot H_2PO_4^-$ (1108.7), $\mathbf{2}\cdot F^-$ (510.4), $\mathbf{2}\cdot AcO^-$ (549.1), $\mathbf{2}\cdot H_2PO_4^-$ (587.0), and $\mathbf{5}\cdot F^-$ (437.1) as well as the corresponding $NDI^{\bullet-}$ radical anions. These data could be rationalized by one of the following scenarios: (1) noncovalent anion/π-acceptor interactions[2,5] leading to anion → NDI ET events[3] that generate $NDI^{\bullet-}$ radical anions and oxidized anions ($X^\bullet$) or (2) NDI−anion covalent bond formation.[5d,7] UV/Vis, NMR, and EPR spectroscopies not only confirm the $NDI^{\bullet-}$ formation via anion → NDI ET events but also rule out NDI−anion covalent bond formation, as the anion-induced and electrochemically generated (anion-free) $NDI^{\bullet-}$ radical anions display essentially identical spectroscopic signatures. The existence of $NDI^{\bullet-}/X^\bullet$ radical pairs (net charge = −1) could be surmised from the ESI-MS data. However, in solutions $X^\bullet$ species do not cause any discernible perturbations of the spectroscopic signatures of the anion-generated $NDI^{\bullet-}$ radical anions, indicating the noncovalent nature of these interactions before, during, and after the ET events. $NOBF_4$ oxidations of $NDI^{\bullet-}$ radical anions regenerate neutral NDIs, but attempts to capture the $X^\bullet$ species with alkenes were inconclusive. It is plausible that the $X^\bullet$ species may act as sacrificial agents[13] that eventually degrade by reacting with solvents, counterions, or themselves, thus preventing the back-ET from $NDI^{\bullet-}$ radical anions. B3LYP/6-31+G** calculations showed that anions preferentially interact with the electron-deficient imide rings of the NDIs (Figure S16).

In conclusion, our studies clearly demonstrate how the interplay between the π-acidity of the NDI and the Lewis basicity of the anion affects the anion/NDI CT and ET interactions. While the more weakly π-acidic NDIs display better selectivity for a strongly basic anion (F^-), the more strongly π-acidic NDIs become promiscuous to different anions. When the thermal anion → NDI ET process is turned OFF because of energy mismatch, light can turn ON the anion → ^{1*}NDI PET pathway, generating the $NDI^{\bullet-}$ radical anions. Light- and electronically gated anion-induced $NDI^{\bullet-}$ formation could be exploited in anion sensing, artificial photosynthesis, catalysis, and molecular electronics.

■ ASSOCIATED CONTENT

Ⓢ Supporting Information. Experimental section and additional experimental and computational results. This material is available free of charge via the Internet at http://pubs.acs.org.

■ AUTHOR INFORMATION

Corresponding Author

saha@chem.fsu.edu

■ ACKNOWLEDGMENT

This work was supported by startup funds from the Florida State University Research Foundation and a FYAP Award.

■ REFERENCES

(1) Njus, D.; Jalukar, V.; Zu, J.; Kelley, P. M. *Am. J. Clin. Nutr.* **1991**, *54*, 1179S.

(2) (a) Rosokha, Y. S.; Lindeman, S. V.; Rosokha, S. V.; Kochi, J. K. *Angew. Chem., Int. Ed.* **2004**, *43*, 4650. (b) Dawson, R. E.; Henning, A.; Weimann, D. P.; Emery, D.; Ravikumar, V.; Montenegro, J.; Takeuchi, T.; Gabutti, S.; Mayor, M.; Mareda, J.; Schalley, C. A.; Matile, S. *Nat. Chem.* **2010**, *2*, 533. (c) Chifotides, H. T.; Schottel, B. L.; Dunbar, K. R. *Angew. Chem., Int. Ed.* **2010**, *49*, 7202.

(3) Guha, S.; Saha, S. *J. Am. Chem. Soc.* **2010**, *132*, 17674.

(4) (a) Lokey, R. S.; Iverson, B. L. *Nature* **1995**, *375*, 303. (b) Iijima, T.; Vignon, S. A.; Tseng, H.-R.; Jarrosson, T.; Sanders, J. K. M.; Marchioni, F.; Venturi, M.; Apostoli, E.; Balzani, V.; Stoddart, J. F. *Chem.—Eur. J.* **2004**, *10*, 6375.

(5) (a) Quiñonero, D.; Garau, C.; Rotger, C.; Frontera, A.; Ballester, P.; Costa, A.; Deyà, P. M. *Angew. Chem., Int. Ed.* **2002**, *41*, 3389. (b) Mascal, M.; Yakovlev, I.; Nikitin, E. B.; Fettinger, J. C. *Angew. Chem., Int. Ed.* **2007**, *46*, 8782. (c) Schottel, B. L.; Chifotides, H. T.; Dunbar, K. R. *Chem. Soc. Rev.* **2008**, *37*, 68. (d) Berryman, O. B.; Johnson, D. W. *Chem. Commun.* **2009**, 3143. (e) Schneider, H.-J. *Angew. Chem., Int. Ed.* **2009**, *48*, 3924.

(6) (a) Bhosale, S. V.; Jani, C. H.; Langford, S. J. *Chem. Soc. Rev.* **2008**, *37*, 331. (b) Sakai, N.; Mareda, J.; Vauthey, E.; Matile, S. *Chem. Commun.* **2010**, *46*, 4225.

(7) (a) Artamkina, G. A.; Egorov, M. P.; Beletskaya, I. P. *Chem. Rev.* **1982**, *82*, 427. (b) Olson, E. J.; Xiong, T. T.; Cramer, C. J.; Bühlmann, P. *J. Am. Chem. Soc.* **2011**, *133*, 12858.

(8) (a) Li, Y.; Flood, A. H. *Angew. Chem., Int. Ed.* **2008**, *47*, 2649. (b) Hay, B. P.; Bryantsev, V. S. *Chem. Commun.* **2008**, 2417.

(9) Gosztola, D.; Niemczyk, M. P.; Svec, W.; Lukas, A. S.; Wasielewski, M. R. *J. Phys. Chem. A* **2000**, *104*, 6545.

(10) Huheey, J. E.; Keiter, E. A.; Keiter, R. L. *Inorganic Chemistry: Principles of Structure and Reactivity*, 4th ed.; Harper Collins: New York, 1993; pp 332−333. A higher Lewis basicity of an anion indicates a greater reducing ability (i.e., a more negative oxidation potential): $F^- > AcO^- > H_2PO_4^- > Cl^- > Br^- > I^-$. Anion's Lewis basicity is solvent-dependent.

(11) Benesi, H. A.; Hildebrand, J. H. *J. Am. Chem. Soc.* **1949**, *71*, 2703.

(12) (a) de Silva, A. P.; Gunaratne, H. Q. N.; Gunnlaugsson, T.; Huxley, A. J. M.; McCoy, C. P.; Rademacher, J. T.; Rice, T. E. *Chem. Rev.* **1997**, *97*, 1515. (b) Flamigni, L.; Collin, J.-P.; Sauvage, J.-P. *Acc. Chem. Res.* **2008**, *41*, 857.

(13) Balzani, V.; Clemente-Léon, M.; Venturi, M.; Credi, A.; Semeraro, M.; Tseng, H.-R.; Wenger, S.; Saha, S.; Stoddart, J. F. *Aust. J. Chem.* **2006**, *59*, 193.